The University of Tehran Press

Pollution

https://jpoll.ut.ac.ir/

Print ISSN: 2383-451X
Online ISSN: 2383-4501

Monitoring Lead Contamination by Integrating Environmental Indices and Random Forest-Based Digital Soil Mapping in Shiraz Urban Watershed, Iran

Amin Mousavi[1]✉ | Sayyed Mahmoud Enjavinezhad[2] | Seyed Javad Naghibi[2,3] | Seyed Kazem Alavipanah[4] | Majid Baghernjad[2] | Ashraf Malekian[5]

1.Department of Soil Science, Ferdowsi University of Mashhad, P.O. Box 9177948978, Mashhad, Iran
2. Department of Soil Sciences, Shiraz University, P.O. Box 71441-13131 Shiraz, Iran
3. Head of Research & Extension Office, Landscape & Green Spaces Organization of Shiraz Municipality, P.O. Box 45366-78 Shiraz, Iran
4. Department of Remote Sensing & GIS, University of Tehran, P.O. Box 14155-6465, Tehran, Iran
5. Department of Agriculture, Payame Noor University, P.O. Box 19395-4697, Tehran, Iran

Article Info

Article type:
Research Article

Article history:
Received: 4 May 2025
Revised: 29 July 2025
Accepted: 7 August 2025

Keywords:
Environmental pollutants
Machine Learning (ML)
Digital mapping
Contamination risk

ABSTRACT

The rapid increase in population and economic expansion has resulted in the infiltration of environmental pollutants, particularly heavy metals, into the soil, presenting a substantial threat to public well-being and reliability of food security. Consequently, awareness and evaluation of these elements are key to assessing soil quality and related risks. In this study, machine learning modeling (random forest model) and digital mapping were employed to quantify and model lead (Pb) contamination using various environmental indices in a section of the urban watershed of Shiraz. For this purpose, 148 soil samples were systematically gathered from a depth of 0 to 20 cm utilizing a randomized sampling approach. After sample preparation, the total Pb content in the soil was determined applying standard analytical methods. Pb contamination risk assessment was conducted using three environmental indices: Geo-Accumulation Index (Igeo), Enrichment Factor (EF), and Contamination Factor (Cf). The results indicated that all analyzed samples exhibited total Pb concentrations (mean: 7.78 mg/kg) below the recommended standard levels for Iran. Based on the Igeo (range: 1.54–4.72), the samples were categorized as moderately to severely contaminated. The EF (range: 4.35–39.65) classified the samples as moderately, highly, and extremely enriched, while the Cf (range: 3.37–29.63) placed the samples in the high to very high contamination category. The interpretation of environmental indices confirmed low to moderate levels of Pb contamination, primarily influenced by anthropogenic activities. Therefore, to ensure sustainable food security, continuous monitoring of Pb concentration variations in the studied soils is essential.

Cite this article: Mousavi, A., Enjavinezhad, S.M., Naghibi, S.J., Alavipanah, S.K., Baghernjad, M., & Malekian, M. (2025). Monitoring Lead Contamination by Integrating Environmental Indices and Random Forest-Based Digital Soil Mapping in Shiraz Urban Watershed, Iran. *Pollution*. 11(4), 1462-1472.
https://doi.org/10.22059/poll.2025.394624.2911

DOI: https://doi.org/10.22059/poll.2025.394624.2911

INTRODUCTION

Soil is a non-renewable resource essential for food production and ecosystem services (Ferreira et al., 2022). Yet, contamination by heavy metals—persistent, low-mobility elements with densities over five times that of water—poses growing risks globally (Ali et al., 2019; Chen et al., 2021; Hammam et al., 2022). In agricultural soils, such contamination, especially by lead (Pb), threatens productivity and food safety. Traditional assessment methods often fall short due to their complexity and cost (Karimi et al., 2017). Digital Soil Mapping (DSM), combining geospatial data and machine learning (ML), offers a more efficient and accurate alternative (McBratney et al., 2003; Minasny & McBratney, 2016; Padarian et al., 2020).

*Corresponding Author Email: *amin_mousavi@alumni.ut.ac.ir*

The integration of remote sensing (RS) and ML has gained prominence in recent years for monitoring soil contamination. Alongside these tools, biological methods such as phytoremediation are proving effective in mitigating heavy metal pollution. For instance, Boukaka and Mayache (2020) showed its potential near a landfill in Algeria, while Nguyen Thanh et al. (2023) demonstrated enhanced chromium uptake in *Solanum nigrum* through bacterial inoculation. Osuntoki et al. (2022) found that petroleum exposure reduced physiological health in cassava. Studies by Fazeli et al. (2019) and Karbassi et al. (2014) further highlighted urban and industrial sources of metal contamination, including traffic emissions and mining activity.

Models like MLR, Cubist, and especially Random Forest (RF) are effective in DSM due to their ability to handle complex, nonlinear data (Zeraatpisheh et al., 2020; Mousavi et al., 2020; Khaledian & Miller, 2020). RF accurately predicts soil properties such as texture, organic matter, bulk density, salinity, and nutrients (Li et al., 2021; Khosravi et al., 2022; Dharumarajan et al., 2022), and DSM is also useful for mapping toxic soil elements (Shahbazi, 2023). Pollution indices like Enrichment Factor (EF), Geo-Accumulation Index (Igeo), and Contamination Factor (C*f*) are key for assessing heavy metal contamination and tracing pollution sources, especially for toxic metals like Pb and Cd (Adnan et al., 2022; Sahraei et al., 2023).

The lack of sufficient data on Pb contamination levels in urban areas, particularly in the urban watershed soils of Shiraz, was one of the main motivations for conducting this study. In these areas, water shortages and farmers' lack of awareness have led to the widespread reliance on urban wastewater for agricultural water supply. Furthermore, the presence of various pollution sources in the city, along with its proximity to a major transportation corridor to southern Iran and heavy vehicular traffic, has significantly related to the accumulation of heavy metal contamination in these regions. Consequently, there is an urgent need to appraise the concentration levels and potential hazards of heavy metals in the soils of these areas.

This study, motivated by limited data on Pb contamination in Shiraz's urban watershed influenced by wastewater irrigation and traffic, applies (1) these three indices to assess Pb risk comprehensively and (2) spatial analysis of Pb distribution, aiming to quantify concentrations and evaluate environmental risks.

MATERIALS AND METHODS

Study area

Figure 1a shows the Shiraz urban watershed in Fars Province, covering about 57203 hectares (UTM 665299–632511 E, 3299803–3271794 N, Zone 39).

Soil sampling and chemical analysis

Using Iso-Cluster classification with maps and expert input (Figure 1b), 148 soil samples (0–20 cm) were randomly collected with GPS. Samples were prepared and total Pb concentrations measured by atomic absorption spectrophotometry using a Shimadzu AA-670 after Aqua Regia acid digestion ($HCl:HNO_3$, 3:1) following Golia et al. (2007).

Utilization of RS data for soil Pb mapping

Using the SCORPAN framework, soil Pb data were integrated with July 2022 Landsat 8 OLI (30 m) and DEM inputs to map Pb distribution. Key RS indices and auxiliary variables used are summarized in Table 1. To improve model accuracy and eliminate redundancy, variables with high multicollinearity (VIF > 10) were excluded (Dormann et al., 2013), followed by Recursive Feature Elimination (RFE) with ten-fold cross-validation, which identified 27 key predictors—including spectral, vegetation, moisture, and topographic features (Table 1)—used in the RF model (Breiman, 2000) in RStudio (v3.5.0).

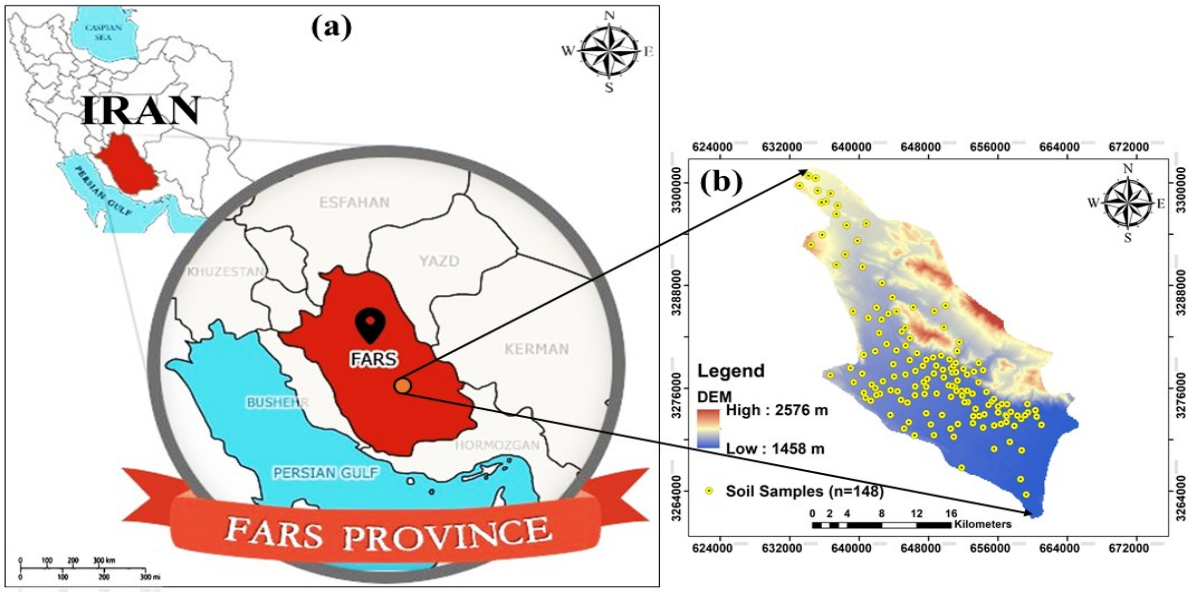

Fig. 1. The study area is located in Fars Province, Iran (a), with the distribution of soil sampling points shown in (b)

Table 1. Environmental covariates applied as predictor in the study area

Covariates (n=27)	Covariate name (abbreviation)	Reference
Topographic attributes	Plan curvature (PlanCurv)	Wilson and Gallant (2000); Gallant and Dowling (2003)
	Profile curvature (ProfCurv)	
	Topographic wetness index (TWI)	
	Multi-resolution valley bottom flatness index (MRVBF)	
	Multi-resolution of ridge top flatness index (MRRTF)	
	Topographic position index (TPI)	Weiss (2001)
RS attributes	Six individual bands (B2, B3, B4, B5, B6, B7)	-
	Principal component analysis of six individual bands (PCA)	(Malone et al., 2009)
	Normalized Difference Vegetation Index (NDVI)	Rouse et al. (1974)
	Soil adjusted vegetation index (SAVI)	(Gilabert et al., 2002)
	Visible Atmospherically Resistant Index (VARI)	(Gitelson et al., 2002)
	Modified Soil-Adjusted Vegetation Index (MSAVI)	(Qi et al., 1994)
	Transformed Vegetation Index (TVI)	McDaniel and Haas (1982)
	Soil Adjusted Total Vegetation Index (SATVI)	(Qi et al., 1994)
	Normalized Difference Moisture Index (NDMI)	(Skakun et al., 2003)
	Normalized Difference Water Index (NDWI)	Xu (2006)
	Modified Normalized Difference Water Index (MNDWI1)	Xu (2006)
	Modified Normalized Difference Water Index (MNDWI2)	Xu (2006)
	Normalized Burn Ratio 1 (NBR1)	(Parks et al., 2014)
	Normalized Burn Ratio 2 (NBR2)	(Parks et al., 2014)
	Salinity Ratio (SR)	(Metternicht and Zinck, 2003)
	Clay Minerals Ratio (CMR)	(Boettinger et al., 2008)

Evaluation of model

To evaluate the performance of the RF model, five statistical criteria were applied: R^2, RMSE, MAE, bias, and CCC. To ensure reliable model evaluation and reduce overfitting, ten-fold cross-validation was employed. In this method, the dataset is divided into ten parts; each subset is used once for validation while the remaining nine are used for training, cycling through all combinations (Kohavi, 1995).

Calculation of soil environmental indices

Pollution indices are widely applied to measure soil contamination and evaluate environmental risks while pinpointing pollution sources (Bali & Sidhu, 2021). This study calculated three such indices: EF, Igeo, and C*f*. To enhance contamination assessment accuracy, regional background values were used. Lacking official geochemical baselines for Shiraz, data from Shakeri et al. (2009) were adopted, reporting natural Pb levels around 6.4 mg/kg in deep, undisturbed soils unaffected by human activity. These rigorously obtained values serve as reliable local references.

Generally, to better understand Pb contamination in the study area, a spatial distribution map was created using the RF method and R 4.4.2 software (R Development Core Team, 2015). Descriptive statistics, including data range and distribution, were analyzed with IBM SPSS Statistics 27.

RESULTS AND DISCUSSION

Descriptive statistical analysis of Pb and environmental indices of soil

This study assessed Pb contamination in soils through pollution factor, Enrichment Factor (EF), and soil accumulation index. Pb levels ranged from 5.12 to 17.40 mg/kg (mean 7.78 mg/kg). The soil accumulation index varied from 1.54 to 4.72 (average 2.74), EF ranged between 4.35 and 39.65 (mean 10.37), and C*f* ranged from 3.37 to 29.63 with an average of 7.85 (Table 2).

Pb contamination across 148 soil samples was assessed using environmental indices. The EF ranged from 4.35 to 39.65 (mean: 10.37), indicating average to very high enrichment and suggesting strong anthropogenic influence (Hamzenejhad, 2020). Igeo values ranged from 1.54 to 4.72 (mean: 2.74), classifying the soils as moderately to extremely polluted. The C*f* varied between 3.37 and 29.63 (mean: 7.85), with 66.66% of sites falling in the highly to very highly polluted range. Overall, the indices point to moderate to severe Pb pollution across the area. The assessment of the three calculated contamination indices, along with field visits to the study area, reveals that anthropogenic activities likely play a notable part in the enrichment of Pb concentrations in the surface soils of the region. Wang et al. (2020) also noted that Pb is primarily influenced by human sources, while Seshan et al. (2010) stated that the use of Igeo and EFs can effectively quantify the scale and severity of soil pollution. Abbasi et al. (2021) found an average Pb concentration of 35.7 mg/kg in dust from Shiraz's 2018 storm, mainly due to industrial and traffic sources. Similarly, our results reveal elevated Pb levels near these areas, supported by EF, Igeo, and C*f* indices indicating significant human impact. Generally, in the

Table 2. Summary of descriptive statistics for measured and predicted parameters in this study (n=148)

Parameters	Min	Max	Mean	25% Quartile	Median	75% Quartile	SD	%CV	Skewness	Kurtosis
Pb (mg/kg)	5.12	17.40	7.78	7.15	7.57	8.38	1.22	15.68	3.29	24.89
EF (Pb)	4.35	39.65	10.37	9.32	10.60	11.43	3.05	29.41	5.77	57.21
Igeo (Pb)	1.54	4.72	2.74	2.63	2.82	2.93	0.35	12.77	-0.16	8.95
C*f* (Pb)	3.37	29.63	7.85	7.07	8.02	8.65	2.27	28.91	5.74	56.80

Table 3. Classification of contamination indices under study

Indices	Range of indices	Soil conditions	References
EF	EF < 2	Minimum enrichment	(Wang et al., 2018)
	EF = 2 − 5	Average enrichment	
	EF = 5 − 20	High enrichment	
	EF = 20 − 40	Very high enrichment	
	EF > 40	Extremely high enrichment	
Igeo	Igeo ≤ 0	Without pollution	(Cai et al., 2019)
	0 ≤ Igeo < 1	Without pollution to moderately polluted	
	1 ≤ Igeo < 2	Moderately polluted	
	2 ≤ Igeo < 3	Moderate to severe pollution	
	3 ≤ Igeo < 4	Severely polluted	
	4 ≤ Igeo < 5	Severely to extremely polluted	
	Igeo > 5	Extremely high pollution	
C*f*	C*f* < 1	Low pollution	(Pendias, 2011)
	1 < C*f* ≤ 3	Moderate pollution	
	3 ≤ C*f* ≤ 6	High pollution	
	C*f* ≤ 6	Very high pollution	

current research, the Cf for Pb exhibited the highest mean value (7.85) among the measured samples, highlighting the significant contribution of anthropogenic activities to environmental contamination (Wieczorek, J & Baran., 2022). The evaluation of pollution concentrations and hazard assessment of heavy metals using the Enrichment Factor (EF) in surface soils of southwestern Shiraz revealed that due to human activities, Pb showed severe enrichment in the research area (Amiri et al., 2022).

Soil Pb contamination and associated risks were evaluated using geochemical indices (Table 3).

Analysis of the spatial variability map of soil Pb contamination

At 148 sites, Pb contamination was assessed. Figure 2a presents the spatial distribution of Pb predicted by the RF model, while Figure 2b illustrates the spatial patterns of Pb concentration (Cf) along with the area coverage for each contamination level

To better understand Pb spatial variability in Shiraz soils, the Cf was used as an integrated pollution index. As shown in Figure 2b, 1.11% of the area was non-contaminated, 27.22% exhibited low contamination, 47.70% moderate, 23.95% moderate-to-high, and 0.02% high contamination. Similar moderate Pb contamination was reported in agricultural soils near Urmia Lake, attributed to intensive fertilizer and pesticide use (Mohammadi et al., 2018). Overall, the results indicated that a significant portion of the study area exhibited considerable Pb enrichment. In other words, human activities, particularly the existence of pollution origins like municipal landfills and wastewater treatment facilities, have played a significant part in shaping the spatial variability of EF (Pb). The mentioned sources remain key contributors to the contamination of PTEs in the region. According to the Iranian Department of Environment (DOE), the acceptable soil Pb limit is 75 mg/kg (Fasihi & Hamidi, 2021). In this study, the average Pb concentration was 7.78 mg/kg, with all 148 samples below this level. Pb levels were also under benchmarks from the Earth's crust, global soils, and standards by Canada, WHO, and USEPA (Table 4). Given the spatial continuity of parent material variations in soils and the localized concentration of environmentally destructive human activities, the relative impact of natural and human-driven factors on heavy metal concentrations across different locations does not exhibit significant variation. Accurate knowledge of the spatial variability patterns of heavy metal concentration levels in soils is a precondition for designing effective control programs (Yang et al., 2009). Due to consistent parent material and localized human impact, Pb showed limited spatial variation. The normal distribution suggests a mainly natural source, consistent

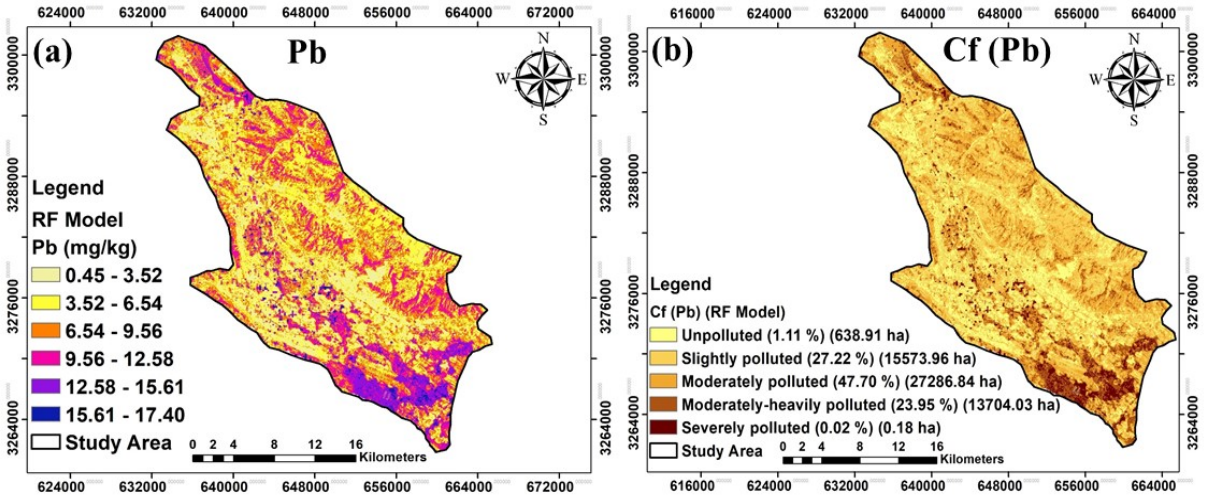

Fig. 2. The spatial variability map of total Pb concentration in the study area using the RF model (a) and the spatial variability of the C*f* (Pb) in the study area along with the corresponding area for each class (b)

Table 4. Total Pb concentration in soil (mg/kg) based on different standards, WHO, USEPA, earth's crust average, global soil average, permissible standard limit – Iran, Canadian Standard

WHO	USEPA	Earth's Crust Average	Global Soil Average	Permissible Standard Limit – Iran	Canadian Standard
30	10	14	35	75	70

with findings by Zhao et al. (2010).

The spatial map shows the highest Pb levels in Shiraz's northern, southern, and southwestern urban watershed areas, mainly due to human activities near highways and heavy traffic zones. Pb accumulation is also linked to wastewater discharge, refineries, agriculture, orchards, and dense residential areas. These results align with Mohammadi et al. (2018) and Mousavi et al. (2022), who identified pesticides, organic fertilizers, wastewater irrigation, and traffic as major Pb sources in soils and water.

Evaluation of RF model performance

The RF model's ability to predict spatial variation of Pb, EF, Igeo, and C*f* was tested using 70% training and 20% test data. Table 5 shows strong performance, with R^2 values near 1 and low RMSE and mean error (ME), confirming high accuracy and reliability. The RF model showed strong predictive power for soil Pb, with an R^2 of 0.87 and low errors (RMSE 0.002, MAE 0.0016), confirming its accuracy and reliability for mapping heavy metal pollution in urban soils. Model evaluation showed minimal bias, with ME near zero, confirming the RF model's accuracy and efficiency. CCC ranged from 0.30 to 0.34—specifically, 0.34 for Pb, 0.32 for EF, 0.31 for Igeo, and 0.30 for C*f*—indicating consistent, unbiased predictions. These findings highlight the RF model's strong performance, supported by RS spectral indices, in mapping soil Pb. The next step involved assessing the importance of model covariates.

Ranking of important covariates in the RF model

The importance of covariates for Pb concentration, EF (Pb), Igeo (Pb), and C*f* (Pb) is illustrated in Figures 3a, 3b, 3c, and 3d, respectively.

For Pb estimation, TVI was the most important, followed by NDWI and MSAVI. NDWI is

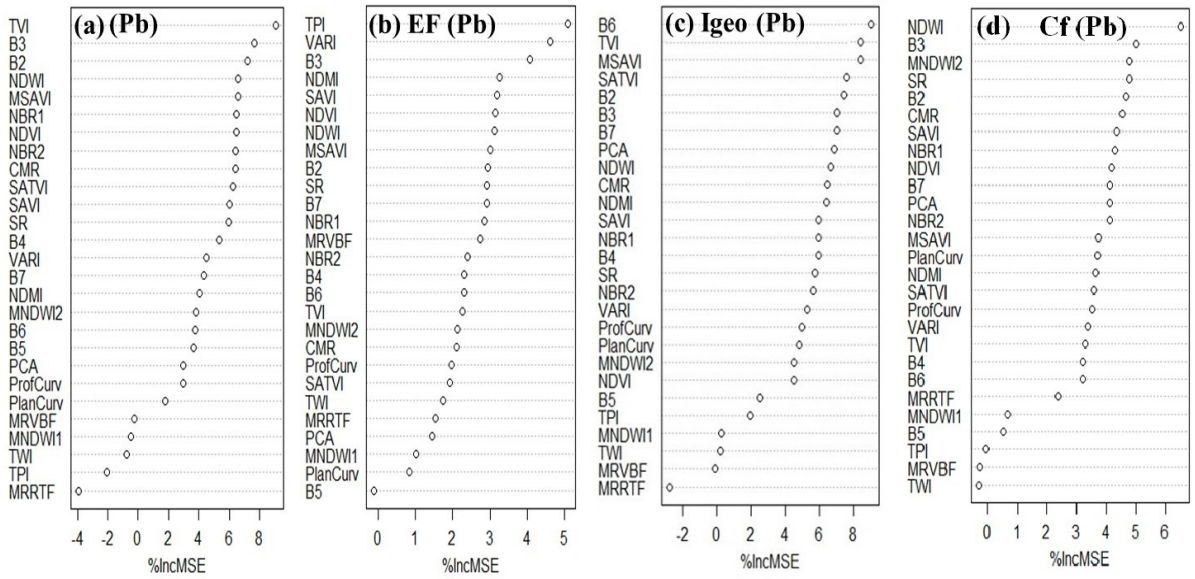

Fig. 3. The prioritized ranking of covariates based on their contribution to the RF model performance Pb (a), EF (Pb) (b), Igeo (Pb) (c) and Cf (Pb) (d), %IncMSE: percent increase of the mean squared error

Table 5. The assessment of modelling performance utilizing statistical metrics in calibration and validation dataset within the study area (n=148)

Parameters	Calibration dataset (n=104) (in the bag)					Validation dataset (n=44) (out of bag)				
	R^2	Concordance	RMSE	MAE	Bias	R^2	Concordance	RMSE	MAE	Bias
Pb	0.87	0.86	0.002	0.0016	0.01	0.27	0.34	0.008	0.0064	0.02
EF ($_{Pb}$)	0.85	0.84	0.005	0.004	0.00	0.26	0.32	0.003	0.0024	0.00
Igeo ($_{Pb}$)	0.84	0.83	0.008	0.0064	0.01	0.25	0.31	0.014	0.0112	0.03
Cf ($_{Pb}$)	0.82	0.81	0.007	0.0056	0.01	0.23	0.30	0.012	0.0096	0.02

calculated from Green and SWIR bands, while MSAVI is derived from NIR and Red bands. For EF (Pb), topographic and vegetation indices such as TPI and VARI, computed from Green, Red, and Blue bands, were the key covariates. For Igeo (Pb), Band 6, topographic and soil-vegetation related indices were the most essential covariates impacting its spatial variability. With regard to Cf (Pb), the impact of NDWI, B3 and MNDWI as a subset of water and individual band 3 were found. For Pb estimation, MSAVI, NBR1, NDVI, and NBR2 were the most influential indices. Among individual bands, Band 4 and Band 7 also played significant roles. The covariate ranking for Pb closely resembled that for EF (Pb). Moisture indices (NDWI, MNDWI2) and geology-related indices (SR, CMR) were key predictors for Cf (Pb). These results highlight the importance of NIR and SWIR spectral regions in metal concentration estimation, consistent with Huang et al. (2020). Vegetation indices like NDVI significantly influenced the prediction of Pb, EF (Pb), and Cf (Pb). As Shi et al. (2021) noted, NDVI is a key factor in digitally mapping zinc (Zn) levels, underscoring how regional conditions strongly affect target variable predictions.

CONCLUTION

This study assessed soil Pb contamination in Shiraz urban watershed using EF, Igeo, and Cf indices. Although average Pb levels were below national and global thresholds, moderate pollution linked to human activities—such as wastewater irrigation, agriculture, traffic, and residential areas—was evident, especially in southern and northeastern zones. The results

highlight the effectiveness of these indices for contamination evaluation and the need for targeted mitigation in affected areas. Future research should use advanced techniques like PCA, PMF, or isotopic fingerprinting to better identify pollution sources from industry, traffic, and agriculture. Combining these tools with spatial mapping and lab tests will improve targeted monitoring. Establishing regional databases and evidence-based management plans is essential for effective soil contamination control.

GRANT SUPPORT DETAILS

The present research did not receive any financial support.

CONFLICT OF INTEREST

The authors declare that there is not any conflict of interests regarding the publication of this manuscript. In addition, the ethical issues, including plagiarism, informed consent, misconduct, data fabrication and/ or falsification, double publication and/or submission, and redundancy has been completely observed by the authors.

LIFE SCIENCE REPORTING

No life science threat was practiced in this research.

REFERENCES

Abbasi, S., Rezaei, M., Keshavarzi, B., Mina, M., Ritsema, C., & Geissen, V. (2021). Investigation of the 2018 Shiraz dust event: Potential sources of metals, rare earth elements, and radionuclides; health assessment. Chemosphere., 279, 130533. https://doi.org/10.1016/j.chemosphere.2021.130533

Adnan, M., Xiao, B., Xiao, P., Zhao, P., Li, R., & Bibi, S. (2022). Research progress on heavy metals pollution in the soil of smelting sites in China. Toxics., 10(5), 231. https://doi.org/10.3390/toxics10050231

Ali, H., Khan, E., & Ilahi, I. (2019). Environmental chemistry and ecotoxicology of hazardous heavy metals: environmental persistence, toxicity, and bioaccumulation. J. Chem., 2019(1), 6730305. https://doi.org/10.1155/2019/6730305

Amiri, H., Daneshvar, E., Azadi, S., & Azadi, S. (2022). Contamination level and risk assessment of heavy metals in the topsoil around cement factory: A case study. Environ. Eng. Res., 27(5). https://doi.org/10.4491/eer.2021.313

Bali, A. S., & Sidhu, G. P. S. (2021). Heavy metal contamination indices and ecological risk assessment index to assess metal pollution status in different soils. In Heavy metals in the environment. Elsevier., (pp. 87-98). https://doi.org/10.1016/B978-0-12-821656-9.00005-5

Boettinger, J.L., Ramsey, R.D., Bodily, J.M., Cole, N.J., Kienast-Brown, S., Nield, S.J., Saunders, A.M. and Stum, A.K. (2008). Landsat spectral data for digital soil mapping. In Digital soil mapping with limited data (pp 193–202). Springer, Dordrecht. https://doi.org/10.1007/978-1- 4020- 8592-5_16

Boukaka, K., & Mayache, B. (2020). Phytoremediation of soil contaminated by heavy metals within a technical landfill center vicinity: Algerian case study. Pollut., 6(4), 811-826. https://doi.org/10.22059/poll.2020.301691.792

Breiman, L. (2001). Random forests. Machine learning, 45, 5-32.

Cai, L. M., Wang, Q. S., Wen, H. H., Luo, J., & Wang, S. (2019). Heavy metals in agricultural soils from a typical township in Guangdong Province, China: Occurrences and spatial distribution. Ecotoxicology and environmental safety, 168, 184-191. https://doi.org/10.1016/j.ecoenv.2018.10.092

Chen, G., Yang, Y., Liu, X., & Wang, M. (2021). Spatial distribution characteristics of heavy metals in surface soil of Xilinguole coal mining area based on semivariogram. ISPRS Int. J. Geo-Inf., 10(5), 290. https://doi.org/10.3390/ijgi10050290

Dharumarajan, S., Lalitha, M., Niranjana, K. V., & Hegde, R. (2022). Evaluation of digital soil mapping

approach for predicting soil fertility parameters—a case study from Karnataka Plateau, India. Arabian J. Geosci., 15(5), 386. https://doi.org/10.1007/s12517-022-09629-8

Dormann, C. F., Elith, J., Bacher, S., Buchmann, C., Carl, G., Carré, G., ... & Lautenbach, S. (2013). Collinearity: a review of methods to deal with it and a simulation study evaluating their performance. Ecography., 36(1), 27-46. https://doi.org/10.1111/j.1600- 0587.2012.07348.x

Fasihi, H., & Hamidi, M. (2020). Investigating the Spread of Soils Pollution and Pollution Sources Originating from Tehran in Rural Districts of Qal'ehno and Kahrizak (Rey Township, Tehran, Iran).

Fazeli, G., Karbassi, A., Khoramnejadian, S., & Nasrabadi, T. (2019). Evaluation of urban soil pollution: a combined approach of toxic metals and polycyclic aromatic hydrocarbons (PAHs). Int. J. Environ. Res., 13, 801-811. https://doi.org/10.1007/s41742-019-00206-8

Ferreira, C. S., Seifollahi-Aghmiuni, S., Destouni, G., Ghajarnia, N., & Kalantari, Z. (2022). Soil degradation in the European Mediterranean region: Processes, status and consequences. Sci. Total Environ., 805, 150106. https://doi.org/10.1016/j.scitotenv.2021.150106

Gallant, J. C., & Dowling, T. I. (2003). A multiresolution index of valley bottom flatness for mapping depositional areas. Water Resour. Res., 39(12). https://doi.org/10.1029/2002WR001426

Gilabert, M. A., González-Piqueras, J., Garcıa-Haro, F. J., & Meliá, J. (2002). A generalized soil-adjusted vegetation index. Remote Sens. Environ., 82(2-3), 303-310. https://doi.org/10.1016/S0034-4257(02)00048-2

Gitelson, A. A., Kaufman, Y. J., Stark, R., & Rundquist, D. (2002). Novel algorithms for remote estimation of vegetation fraction. Remote Sens. Environ., 80(1), 76-87. https://doi.org/10.1016/S0034-4257(01)00289-9

Golia, E. E., Tsiropoulos, N. G., Dimirkou, A., & Mitsios, I. (2007). Distribution of heavy metals of agricultural soils of central Greece using the modified BCR sequential extraction method. Int. J. Environ. Anal. Chem., 87(13-14), 1053-1063. https://doi.org/10.1080/03067310701451012

Hammam, A. A., Mohamed, W. S., Sayed, S. E. E., Kucher, D. E., & Mohamed, E. S. (2022). Assessment of soil contamination using gis and multi-variate analysis: A case study in El-Minia Governorate, Egypt. Agronomy., 12(5), 1197. https://doi.org/10.3390/agronomy12051197

Hamzenejhad, R. (2020). Quantitative assessment of soil heavy metals pollution. Appl. Soil Ecol., 8(2), 37-52.

Huang, H., Zhou, Y., Liu, Y., Li, K., Xiao, L., Li, M., ... & Wu, F. (2020). Assessment of anthropogenic sources of potentially toxic elements in soil from arable land using multivariate statistical analysis and random forest analysis. Sustainability., 12(20), 8538. https://doi.org/10.3390/su12208538

Karbassi, A., Nasrabadi, T., Rezai, M., & Modabberi, S. (2014). Pollution with metals (As, Sb, Hg, Zn) in agricultural soil located close to Zarshuran gold mine, Iran. EEMJ., 13(1). https://doi.org/10.30638/eemj.2014.014

Karimi, A., Haghnia, G. H., Ayoubi, S., & Safari, T. (2017). Impacts of geology and land use on magnetic susceptibility and selected heavy metals in surface soils of Mashhad plain, northeastern Iran. J. Appl. Geophys., 138, 127-134. https://doi.org/10.1016/J.JAPPGEO.2017.01.022

Khaledian, Y., & Miller, B. A. (2020). Selecting appropriate machine learning methods for digital soil mapping. Appl. Math. Modell., 81, 401-418. https://doi.org/10.1016/j.apm.2019.12.016

Khosravi, M., Zolfaghari, A., Kaboli, S. H., & Ghafari, H. (2022). Application of digital soil mapping in soil particle size zonation and estimation of saturated soil hydraulic conductivity for optimal management of watersheds (case study: Damghanrood Watershed). Iran. J. Soil Water Res., 53(2), 245-261. https://doi.org/10.22059/IJSWR.2022.333013.669113

Kohavi, R. (1995). A study of cross-validation and bootstrap for accuracy estimation and model selection. IJCIA., 14(2), 1137-1145.

Li, X., Ding, J., Liu, J., Ge, X., & Zhang, J. (2021). Digital mapping of soil organic carbon using sentinel series data: a case study of the Ebinur lake watershed in Xinjiang. Remote Sens., 13(4), 769. https://doi.org/10.3390/rs13040769

Lin, I. (1989). A concordance correlation coefficient to evaluate reproducibility. Biom., 45, 255-268.

Malone, B. P., McBratney, A. B., Minasny, B., & Laslett, G. M. (2009). Mapping continuous depth functions of soil carbon storage and available water capacity. Geoderma., 154(1-2), 138-152. https://doi.org/10.1016/j.geoderma.2009.10.007

McBratney, A. B., Santos, M. M., & Minasny, B. (2003). On digital soil mapping. Geoderma., 117(1-2), 3-52. https://doi.org/10.1016/S0016-7061(03)00223-4

McDaniel, K. C., & Haas, R. H. (1982). Assessing mesquite-grass vegetation condition from Landsat.

Photogramm. Eng. Remote Sens., 48(3), 441-450.
Metternicht, G. I., & Zinck, J. A. (2003). Remote sensing of soil salinity: potentials and constraints. Remote Sens. Environ., 85(1), 1-20. https://doi.org/10.1016/S0034-4257(02)00188-8
Minasny, B., & McBratney, A. B. (2016). Digital soil mapping: A brief history and some lessons. Geoderma., 264, 301-311. https://doi.org/10.1016/j.geoderma.2015.07.017
Mohammadi, A., Hajizadeh, Y., Taghipour, H., Mosleh Arani, A., Mokhtari, M., & Fallahzadeh, H. (2018). Assessment of metals in agricultural soil of surrounding areas of Urmia Lake, northwest Iran: A preliminary ecological risk assessment and source identification. Hum. Ecol. Risk Assess.: Int. J., 24(8), 2070-2087. https://doi.org/10.1080/10807039.2018.1438173
Mousavi, A., Shahbazi, F., Oustan, S., Jafarzadeh, A. A., & Minasny, B. (2020). Spatial distribution of iron forms and features in the dried lake bed of Urmia Lake of Iran. Geodermal Reg., 21, e00275. https://doi.org/10.1016/j.geodrs.2020.e00275
Mousavi, S. M., Brodie, G., Payghamzadeh, K., Raiesi, T., & Strivastava, A. K. (2022). Lead bioavailability in the environment: its exposure and and effects. JAEHR., 10(1), 1-14. https://doi.org/10.32598/JAEHR.10.1.1256
Nguyen Thanh, H., Nguyen Thi Ngoc, H., & Mai Huong, T. (2023). Effective combination of *Lysinibacillus sphaericus* and phytoremediation in soil contaminated with chromium. Pollut., 9(1), 15-22. https://doi.org/10.22059/poll.2022.335374.1287
Osuntoki, A., Olukanni, O., Nwakile, O., & Kabiru, A. (2022). Oxidative Stress Induction in Cassava Plant (Manihot Esculenta Crantz) Grown on Soil Contaminated with Diesel. Pollut., 8(2), 671-679. https://doi.org/10.22059/poll.2022.331299.1197
Padarian, J., Minasny, B., & McBratney, A. B. (2020). Machine learning and soil sciences: A review aided by machine learning tools. Soil, 6(1), 35-52. https://doi.org/10.5194/soil-6-35-2020
Parks, S. A., Dillon, G. K., & Miller, C. (2014). A new metric for quantifying burn severity: the relativized burn ratio. Remote Sens., 6(3), 1827-1844. https://doi.org/10.3390/rs6031827
Pendias, A. K. (2011). Trace elements in soils and plants. (p. 548) (Verenigde Staten: CRC press). https://doi.org/10.1201/b10158
Peng, Y., Kheir, R. B., Adhikari, K., Malinowski, R., Greve, M. B., Knadel, M., & Greve, M. H. (2016). Digital mapping of toxic metals in Qatari soils using remote sensing and ancillary data. Remote Sens., 8(12), 1003. https://doi.org/10.3390/rs8121003
Qi, J., Chehbouni, A., Huete, A. R., Kerr, Y. H., & Sorooshian, S. (1994). A modified soil adjusted vegetation index. Remote Sens. Environ., 48(2), 119-126. https://doi.org/10.1016/0034-4257(94)90134-1
R Development Core Team. (2015). R: a language and environment for statistical computing. R. Foundation for Statistical Computing, Vienna, Austria.
Rouse, J. W., Haas, R. H., Schell, J. A., and Deering, D. W. (1974, December). Monitoring vegetation systems in the Great Plains with ERTS. (Paper presented at the Third Earth Resources Technology Satellite Symposium, Greenbelt, NASA SP-351, Vol. 30103017, p. 317)
Sahraei, N., Landi, A., Hojati, S., & Pasolli, E. (2023). Assessment of pollution in the central soils of Khuzestan province with potentially toxic elements (PTEs) and their origins. Water and Soil., 37(3), 457-471. https://doi.org/10.22067/jsw.2023.81161.1254
Seshan, B. R. R., Natesan, U., & Deepthi, K. (2010). Geochemical and statistical approach for evaluation of heavy metal pollution in core sediments in southeast coast of India. IJEST., 7, 291-306. https://doi.org/10.1007/BF03326139
Shahbazi, F., Weber, T. K. D., Oustan, S., Alvyar, Z., Jeon, S., & Minasny, B. (2023). Uncovering the effects of Urmia Lake desiccation on soil chemical ripening using advanced mapping techniques. Catena., 232, 107440. https://doi.org/10.1016/j.catena.2023.107440
Shakeri, A., Moore, F., & Modabberi, S. (2009). Heavy metal contamination and distribution in the Shiraz industrial complex zone soil, South Shiraz, Iran. World Appl. Sci. J., 6(3), 413-425.
Skakun, R. S., Wulder, M. A., & Franklin, S. E. (2003). Sensitivity of the thematic mapper enhanced wetness difference index to detect mountain pine beetle red-attack damage. Remote Sens. Environ., 86(4), 433-443. https://doi.org/10.1016/S0034-4257(03)00112-3
Wang, J., Zhang, X., Yang, Q., Zhang, K., Zheng, Y., and Zhou, G. (2018). Pollution characteristics of atmospheric dustfall and heavy metals in a typical inland heavy industry city in China. Journal of Environmental Sciences, 71, 283-291. https://doi.org/10.1016/j.jes.2018.05.031
Wang, Y., Duan, X., & Wang, L. (2020). Spatial distribution and source analysis of heavy metals in soils influenced by industrial enterprise distribution: Case study in Jiangsu Province. Sci. Total Environ.,

710, 134953. https://doi.org/10.1016/j.scitotenv.2019.134953
Weiss, A. (2001, July). Topographic position and landforms analysis. (Poster presented at the ESRI User Conference, Vol. 200, San Diego, CA).
Wieczorek, J., & Baran, A. (2022). Pollution indices and biotests as useful tools for the evaluation of the degree of soil contamination by trace elements. J. Soils Sediments., 1-18. https://doi.org/10.1007/s11368-021-03091-x
Wilson, J. P., & Gallant, J. C. (2000). Digital terrain analysis. Terrain analysis: Principles and applications, 6(12), 1-27. (ISBN: 978-0-471-32188-0)
Xu, H. (2006). Modification of normalised difference water index (NDWI) to enhance open water features in remotely sensed imagery. Int. J. Remote Sens., 27(14), 3025-3033. https://doi.org/10.1080/01431160600589179
Yang, P., Mao, R., Shao, H., & Gao, Y. (2009). The spatial variability of heavy metal distribution in the suburban farmland of Taihang Piedmont Plain, China. C. R. Biol., 332(6), 558-566. https://doi.org/10.1016/j.crvi.2009.01.004
Zeraatpisheh, M., Ayoubi, S., Jafari, A., Tajik, S., & Finke, P. (2019). Digital mapping of soil properties using multiple machine learning in a semi-arid region, central Iran. Geoderma., 338, 445-452. https://doi.org/10.1016/j. geoderma.2018.09.006
Zhao, Y., Wang, Z., Sun, W., Huang, B., Shi, X., & Ji, J. (2010). Spatial interrelations and multi-scale sources of soil heavy metal variability in a typical urban–rural transition area in Yangtze River Delta region of China. Geoderma., 156(3-4), 216-227. https://doi.org/10.1016/j.geoderma.2010.02.020